Journal Pre-proof

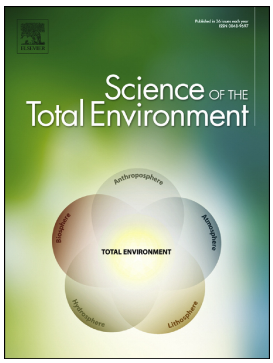

Adsorption of toluene on various natural soils: Influences of soil properties, mechanisms, and model

Yuan Li, Mingli Wei, Lei Liu, Qiang Xue, Bowei Yu

PII: S0048-9697(20)33624-X

DOI: https://doi.org/10.1016/j.scitotenv.2020.140104

Reference: STOTEN 140104

To appear in: *Science of the Total Environment*

Received date: 16 March 2020

Revised date: 6 June 2020

Accepted date: 8 June 2020

Please cite this article as: Y. Li, M. Wei, L. Liu, et al., Adsorption of toluene on various natural soils: Influences of soil properties, mechanisms, and model, *Science of the Total Environment* (2020), https://doi.org/10.1016/j.scitotenv.2020.140104

Adsorption of Toluene on Various Natural Soils: Influences of Soil Properties, Mechanisms, and Model

Yuan Li [a, b, c, d], **Mingli Wei** [a, c, d, e] *, **Lei Liu** [a, c, d, e], **Qiang Xue** [a, c, d, e], **Bowei Yu** [f]

[a] State Key Laboratory of Geomechanics and Geotechnical Engineering, Institute of Rock and Soil Mechanics, Chinese Academy of Sciences, Wuhan, 430071, China

[b] University of Chinese Academy of Sciences, Beijing, 100000, China

[c] IRSM-CAS/HK Poly U Joint Laboratory on Solid Waste Science, Wuhan, 430071, China

[d] Hubei province Key Laboratory of contaminated sludge and soil science and Engineering, Wuhan, China

[e] Jiangsu Institute of Zoneco Co., Ltd., Yixing, 214200, China

[f] School of Civil Engineering, University of Sydney, 2008, Australia

Abstract: This study investigated toluene adsorption on natural soils. The linear partition model was found to represent the adsorption isotherm well (R^2 = 0.958-0.994), compared with the Freundlich model (R^2 = 0.901-0.991). Therefore, the coefficient, K_d, of the linear model indicated the adsorption capacity of soils A to F. Traditionally, K_d and the total organic carbon (TOC) content have a good linear relationship. However, this relationship was weak (correlation coefficient (r) = 0.689) when TOC values (8.43-12.9 mg/g) were low and close. To correct this

* Corresponding author.

deviation, this study investigated the influences of physicochemical properties, such as special surface area, mineral composition, functional groups, pH, and potentials. As soils B and C consisted of a large amount of active clayey minerals (69.4% kaolinite and 79.3% nacrite, respectively) and rich functional groups, they demonstrated the strongest adsorption capacity. Additionally, the *r* for pH-K_d, zeta potential-K_d, and redox potential-K_d were high, at 0.806, 0.914, and 0.932, respectively. To explore adsorption mechanisms, the adsorption thermodynamic parameter (enthalpy) was used initially to determine the forces. Combined with the analysis of soil properties, the mechanisms identified were hydrophobic interaction and hydrogen-pi bonding, involving co-adsorption with water molecules. Based on all studies, the properties were quantified and simplified by the plastic limit (PL), and TOC was simplified by soil organic matter (SOM). Then, PL and SOM were weighted by the entropy-weight method to obtain the determination factor, *DF*, a logarithmic parameter to replace TOC. Finally, a new model describing toluene adsorption on natural soils was established and expressed as $K_d = 4.80+3.53DF$. This new model had significantly improved the correlation between K_d and TOC (r=0.933) and expanded the engineering adaptability.

Keywords: toluene adsorption, soil properties, thermodynamics, mechanism, model

1 Introduction

Contamination in soils has caused alarming issues in ecosystems and human health worldwide. Complex organic pollutants are monitored in densely populated and highly industrialized areas (Sun et al., 2018). The characteristics of organic pollutants, such as high toxicity, strong persistence, high spatial heterogeneity, and possible bioconcentration, make them

priorities in soil contamination research (Cheng et al., 2019). In recent years, with the extensive production, consumption, and leaking of petroleum products worldwide, the benzene series (BTEX), especially toluene, have been classified as priority pollutants in contaminated soils and have been the focus of recent research (Balseiro-Romero et al., 2018; Gholami et al., 2019; Hunt et al., 2019).

Toluene is a representative hydrophobic organic pollutant (HOP) and is a long-term source of soil and aquifer contamination (Long et al., 2013). Toluene has been regulated in many countries, e.g., China, the USA, the UK, and the Netherlands (Sun et al., 2020; Swartjes et al., 2012). In China, as the dominant BTEX pollutant, toluene accounted for approximately 41.6% and 32.1% of total contamination cases in agricultural soils in 2013 and 2016, respectively (Xu et al., 2019). Contaminants penetrate the ground, adsorb on natural soils, and act as a potential pollution source. Understanding the adsorption behaviors that will reflect the content and distribution of pollutants is key to dealing with this contamination (Essaid et al., 2015; Ye et al., 2017). This understanding will influence the choice and optimization of soil vapor extraction, thermal desorption, chemical oxidation, or other methods (Agarwal and Liu, 2015; Lim et al., 2016; Suanon et al., 2020; Vidonish et al., 2016). Generally, an accurate understanding of the adsorption process aims to address three issues in any remediation project: the determination of the contamination plume, process optimization of the remediation method, and resolution of the tailing effects (Moyo et al., 2014).

Adsorption behaviors have been intensively investigated in recent decades. Whilst the effect of total organic carbon (TOC) on toluene adsorption has been studied in depth, understanding of the influence of soil physicochemical properties on this aspect is still lacking. Zytner (1994)

suggested that soils with higher TOC content exhibited higher adsorption with BTEX. Xing (2001) found that TOC influenced adsorption mechanisms and suggested that organic pollutants were adsorbed in expanded and condensed domains of TOC. They also found that the specific components of TOC, e.g., humic acid (HA), fulvic acid (FA), and protein, also influence adsorption (Chiou et al., 2000; Payá-Pérez et al., 1992). Some studies have focused on exploring the linear relationship between soil adsorption capacities and TOC contents (Balseiro-Romero et al., 2018; Joo et al., 2011; Karickhoff et al., 1979; Martz et al., 2019); these revealed that TOC could be an indicator to evaluate soil adsorption behavior. On the other hand, some researchers explored the influences of soil physical properties, e.g., clayey minerals, specific surface area (SSA), particle size distribution, porosity feature, on soil adsorption behavior (Adeyinka and Moodley, 2019; Deng et al., 2017). However, there were few studies on the influences of pH, zeta potential, redox potential, and other chemical characteristics on soil adsorption behavior (Gondar et al., 2013; Hunter, 1981; Plaza et al., 2015; You et al., 1999).

It is questionable whether the single factor of TOC may be used for on-site determination of soil adsorption capacity of HOPs (Chen et al., 2007; Joo et al., 2011; Martz et al., 2019). Natural soils typically have low TOC contents, and their values vary in small ranges, especially for soils in deeper areas (Essaid et al., 2015; Liang et al., 2019). In these cases, the influences of HA, FA, and other factors are also limited by low TOC content. The TOC prediction model of China based on the second national soil survey showed that from 0 to 2 m, the highest TOC content was 18.9 mg/g (surface soil), and the lowest was 5.9 mg/g (deep soil), decreasing with an increase in depth (Liang et al., 2019). Therefore, as the adsorption behaviors may notably vary in different soils (Awad et al., 2019; Moyo et al., 2014), deviations are expected when determining the soil adsorption

capacity solely based on TOC contents and types. Under these conditions, there should be a focus on the soil itself.

Therefore, the objectives of this study are to discuss toluene adsorption on natural soils with different properties, analyze its adsorption mechanisms, and establish a new model to eliminate deviations. First, correlations between toluene adsorption and various soil parameters, including SSA, pH, redox potential, and zeta potential, were established. Microanalysis tests such as X-ray diffraction (XRD) and Fourier transform infrared reflection (FTIR), were included in the investigation to assess the influences of mineral composition and functional groups. Second, adsorption mechanisms were analyzed based on adsorption thermodynamics and multiscale tests. Finally, an adsorption capacity model that considers the influences of soil properties was established. This model could provide accurate predictions on toluene adsorption for soils with close TOC contents.

2 Materials and methods

2.1 Materials

2.1.1 Soils

Six batches of soils named A to F, collected from the ground surface (10-20 cm depth), were included in the study, as listed in Table A.1 (Appendix). The collected soils were air-dried at room temperature for a month and then ground to powders passing through a 2-mm mesh. Toluene was not detected in these soils. Soils were then exposed to ultraviolet (UV) radiation to reduce biological activity before experiments. The parameters of the UV light source are listed in Table B.1 (Appendix).

The basic physical properties of the collected soils were tested. Soil properties, e.g., limit

moisture, specific gravity, and particle size analysis, were tested as per the Chinese national standard GB/T 50123-2019 (MOHURD, 2019). The organic matter content was determined according to the methods given by ASTM D2974-14 (ASTM, 2014). The TOC content of soils was measured using a Vario TOC analyzer (Elementer, Germany). The SSA and pore volumes were tested using the Brunauer, Emmett and Teller (BET) method, with the ASAP 2020 PLUS HD88 analyzer (Micromeritics, USA). The XRD tests on the soils were carried out using a D8-Advance XRD diffractometer (Bruker, Germany) to determine the mineral composition. The qualitative and quantitative analyses of the XRD results were conducted using the DIFFRAC EVA software with the PDF 2004 database (Mora et al., 2014). The structure of the functional groups in the soils was investigated using the FTIR spectrometer (Thermo Fisher, USA) with the spectral range of 400 to 4000 cm^{-1}.

The chemical properties of the soils were also tested. The determination of soil pH was carried out as per ISO 10390: 2005, using a PHS-3E pH meter (Leici, China). In the tests, the soil/water ratio was altered to 1:10 to maintain consistency with the ratio used in the batch adsorption experiment. Soil-water mixtures were also used to determine the redox and zeta potentials. The redox potentials were measured by a PHS-3E meter with an ORP electrode (Leici, China). The zeta potentials were tested using a Nano NS-90 zetasizer (Malvern, UK). The physicochemical properties of the soils are summarized in Table 1.

Furthermore, the redox and zeta potentials were also tested for the soils that were later mixed with toluene (Appendix, Table C.1). The adsorbate used was the stock solution (20 mg/L, Section 2.1.2).

2.1.2 Chemical reagents

The chemical reagents, toluene (≥99.5%), and anhydrous calcium chloride (≥96.0%), were supplied by Sinopharm Chemical Reagent Co. Ltd. (Shanghai, China). The internal and surrogate standards were provided by the o2si Standards Company (Charleston, USA). Milli-Q water (Merck Millipore, Germany) was used in this study.

A 0.01 mol calcium chloride (increase centrifugation) and 20 mg of toluene were added into a 1 L volumetric flask, and Milli-Q water was used to fix this volume to prepare the stock solution with a concentration of 20 mg/L. The stock solution was vigorously mixed and then sealed with parafilm (Bemis Company, Inc., USA) and stored in a 4 °C refrigerator in the dark.

2.2 Test Methodology

2.2.1 Batch adsorption experiment

Batch adsorption experiments for soils A to F were conducted in 50 mL polypropylene centrifuge tubes. Three identical specimens of each type of soil were tested. The testing process followed the Chinese national standard GB/T 21851-2008 (same as OECD 106 standard) (SAC, 2008) and methods described in the literature (Garoma and Skidmore, 2011; Zytner, 1994). The solid to liquid ratio was set at 1:10 (g/mL) to ensure the soil adsorption capacity was between 20% and 85%. Five grams of soil were first suspended in a 50 mL toluene solution (concentrations were 0.2, 2, 4, 8, and 12 mg/L) in the centrifuge tubes. These tubes were kept in a DKZ-3 constant temperature oscillator (Shanghai, China) at a speed of 200 rpm and a temperature of 23±2°C (Garoma and Skidmore, 2011). The equilibration time was set as 24 h, based on the literature (Garoma and Skidmore, 2011; Li and Gupta, 1994). A control group was tested where tubes only contained toluene solutions in those five concentrations without soils. The control group was able to balance the loss of toluene. During the tests, all tubes were sealed with parafilm. After the

adsorption equilibrium, tubes were centrifuged at 3000 G for 30 min. The supernatant was filtered, diluted to 100 μg/L, and stored in 40 mL VOA vials for further tests.

In addition to the adsorption isotherms at 296 K (23 °C), adsorption isotherms at 306 and 316 K were also obtained. Therefore, thermodynamic parameters were calculated by three sets of adsorption isotherms at different temperatures. The calculation process showed in Appendix (Part D).

2.2.2 Gas chromatography and mass spectrometry tests

To test toluene concentration, the supernatant in vials was added 10 μl internal standard and 10 μl surrogate standard and analyzed by 7890A gas chromatography-5975C mass spectrometry (GC-MS, Agilent, USA) with Atomx XYZ purge and trap autosampler (Tekmar, USA). The room temperature kept at 23±1 °C during the measurement. The working conditions of GC-MS and the autosampler referenced the China environmental protection standard (HJ 605-2011).

3 Results and Analysis

3.1 Isothermal Adsorption Characters of Soils

Adsorption isotherm models were used to describe the adsorption capacity of toluene on natural soils in this study. Table E.1 (Appendix) lists two commonly used adsorption isotherm models, the Freundlich and linear partition models, to describe the adsorption equilibrium of toluene within a low concentration range (Pino-Herrera et al., 2017).

The fitting parameters of the Freundlich and linear partition models are shown in Table 2. The R^2 of the two models applied on soils A to F suggested that the linear partition model fitted the adsorption better compared to the Freundlich model. Therefore, K_d of the linear partition adsorption was represented as the adsorption capacity and adopted in correlations with other soil

characteristics. Actually, the parameters 1/*n* in the Freundlich model of most soils were close to 1, which meant that the nonlinear behavior of toluene adsorption on soils was not visible (Carmo et al., 2000). The nonlinearity was believed to result from the adsorption on organic carbon with a high specific surface area (Chiou et al., 2000). The TOC contents of soils A-F were low, and as such, nonlinearity was poor. Meanwhile, the better effect of the linear partition model illustrated that other weak forces, such as hydrophobic interaction and weak hydrogen bonding, could also contribute to toluene adsorption on soil surfaces (Su et al., 2006).

Generally, a larger K_d increases the adsorption capacity. Based on K_d values from Table 2, the order of toluene adsorption capacities of soil A to F was B > C > D > E > A > F. Soil B exhibited the strongest adsorption for toluene. The differences between adsorbent (natural soils) performances were subsequently carefully analyzed according to the soil physicochemical properties.

3.2 Analysis of Minerals and Functional Groups

The XRD spectra of soils A to F are shown in Fig. 1, and the main mineral composition of soils is shown in Table 3. In Fig. 1, both kaolinite (K) and nacrite (N) belong to the kaolinite minerals. The rectorite (R) is the 1:1 interstratified mineral composed of dioctahedral mica and dioctahedral smectite. Microcline (M) and albite (AL) are both feldspar minerals. However, M is a potassium-containing aluminosilicate, and the AL is a sodium-containing aluminosilicate. Birnessite (BI) is an alkaline manganese oxide mineral.

Table 3 shows that most soils were mainly composed of quartz (Q), with the exception of soils B and C (containing 69.4% K and 79.3% N, respectively). Comparatively, soil D contained 24.8% R, and soil E contained only 29.2% AL. Soil E did not include kaolinite, and soil A and F

had the worst adsorption capacity; neither of them contained clayey minerals. Soil A contained 18.8% AL, while soil F contained only 8.9% AL. Detailed XRD quantitative analysis results for each soil are shown in Fig. F.1-F.6 (Appendix).

Fig. 2 shows the FTIR spectra of soil A to F before and after adsorption. The broad peak between 3345-3385 cm^{-1} shown in each spectrum was the hydroxyl stretching vibration of water molecules (Hu et al., 2019). The peak at approximately 1636 cm^{-1} was the bending vibration of hydroxyl in water molecules (Woolverton and Dragila, 2014) and the stretching of aromatic C=C in the soils (Xing et al., 2019).

Alongside the XRD results, the FTIR spectra of natural soils were also analyzed. In soils B and C, peaks around 3691, 3619, 1027, 1000, and 910 cm^{-1} indicated the presence of kaolinite. Specifically, peaks at approximately 3691cm^{-1} (3690 and 3691 cm^{-1}) and around 910 cm^{-1} (908 and 910 cm^{-1}), were the stretching vibration of the aluminol group (Al-OH) in kaolinite (Nayak and Singh, 2007). Peaks at 3619 cm^{-1} were the -OH stretching vibration of kaolinite (Nguyen et al., 1991). Meanwhile, peaks at 1027 cm^{-1} and around 1000 cm^{-1} (996 and 1004 cm^{-1}), were the stretching vibration of the siloxane (Si-O) of kaolinite. For soil D, 1000 cm^{-1} was the stretching vibration of siloxane (Si-O) (Hu et al., 2019). In soil E, 995 cm^{-1} was the stretching vibration of the Si-O of albite, and 779 cm^{-1} was the stretching vibration of quartz (Bernier et al., 2013). In natural soils A and F, 1000 cm^{-1} was the characteristic peak of quartz.

Compared with natural soils and the adsorbed soils of the FTIR spectra, we observed that the wavenumber of peaks at approximately 3600, 1000, and 900 cm^{-1}, decreased after toluene adsorption. This illustrated that the vibrational frequencies of functional groups such as siloxane (Si-O), silanol (Si-OH), and aluminol (Al-OH) became lower.

3.3 Correlations of Soil Adsorption and Basic Soil Properties

3.3.1 Physical properties

The SSA was one of the critical physical properties for adsorption, and to a certain extent, it also reflected other properties, e.g., particle size distribution, pore volume, and pore distribution. However, as shown in Fig. G.1 (Appendix), the correlation of K_d-SSA was very poor (r was 0.0433, and the p-value was 0.339>0.05). This indicated that SSA was not a dominant soil property influencing toluene adsorption on natural soils. In other words, the effect of SSA on toluene adsorption was negligible. There was no traditional understanding that adsorption capacity increased with the increase of SSA because these references used soils after particle size grouping or pure minerals as objects (in these cases, there was a significant magnitude difference in SSA) (Adeyinka and Moodley, 2019; Pino-Herrera et al., 2017). Carmo et al. (2000) came to a similar conclusion that there was no correlation between the SSA and the adsorption capacity of naphthalene or phenanthrene (R^2 was 0.17 and 0.09, respectively). In general, this phenomenon reflects that toluene was unevenly adsorbed on the solid-liquid interface, and may adhere to specific adsorption sites in natural soils (Li et al., 2019).

Therefore, further exploration on other properties affecting toluene adsorption and mechanisms is required. The results of the XRD and FTIR analyses represent the correlation of soil adsorption and mineral composition. The order of adsorption capacities may be reflected in the mineral composition and content of these soils, as suggested by the quantitative XRD analysis. Compared to other minerals, the clayey minerals of K, N, and R in soil B-D exhibited higher activity, larger hydrophobic surface, and a greater number of active functional groups (Lambert, 2018; Yin et al., 2012). Soils B and C had the strongest adsorption capacity with regard to toluene,

and they both contained higher clayey minerals compared to other soils. Contact angle measurements showed that the silica tetrahedral surface in kaolin had certain hydrophobicity (Du and Miller, 2007; Hunter, 1981; Yin et al., 2012), which was stronger than that of illite/muscovite (Durand and Rosenberg, 1998). The slightly higher adsorption capacity of soil B than C was because N of soil C was very stable due to its crystalline structure and had a less hydrophobic surface. Meanwhile, M in soil B belonged to aluminosilicate minerals, so hydrophobic adsorption of toluene may occur on the surface of the siloxane tetrahedron (Xu et al., 2018). Therefore, M exhibited stronger hydrophobic adsorption than quartz. The reduced adsorption of toluene in soils D and E, compared to soils B and C, was due to the R and AL in these two soils, respectively, wherein there was reduced content of R and AL was not a clayey mineral. The AL in soils A, E, and F had less adsorption capacity for toluene than clayey minerals (Awad et al., 2019; Xu et al., 2018). As such, the order of adsorption capacity for soils A, E, and F were same as that of AL content.

Furthermore, Fig. 2 shows that these functional groups could provide adsorption sites for toluene. It was because toluene adsorption for these functional groups occurred through hydrophobic interaction and weak hydrogen bond, resulting in a lower vibrational frequency and energy of siloxane, silanol, and aluminol. All soils had siloxane (Si-O) surfaces (at approximately 1000 and 900 cm^{-1}), illustrating that they all had a certain adsorption capacity. The capacity differences may depend on mineral surface activity, similar to XRD analysis. Particularly, soils B and C with -OH (about 3600 cm^{-1}) were also favorable for toluene adsorption through a weak hydrogen bond. Therefore, its adsorption mechanisms were more abundant, showing that they performed better than other soils.

3.3.2 Chemical properties

The correlations of adsorption and some chemical properties are shown in Fig. 3. Fig. 3a shows the linear relationship between soil pH and their K_d values. The K_d decreased when the pH increased. Specifically, soil B had a pH of 7 and exhibited the strongest adsorption of toluene. The blue line in Fig. 3a is the fitting only for neutral or alkaline soils, showing a better effect (correlation coefficient r was 0.991, p = 7.39e-6<0.05), compared to the red line (containing acid soil C, r = 0.806 and p = 8.18e-5<0.05). The results showed that there was a strong correlation between soil adsorption and pH, mainly when the soil was neutral or weakly alkaline. These results were consistent with those of Ertli et al. (2004) and Flores et al. (2009), and indicated that the hydrophobic interactions were weaker in alkaline environments compared to neutral or acidic environments. The weak hydrogen bond between the toluene and functional groups became weaker under alkaline conditions (Ertli et al., 2004). With an increase in pH, large amounts of TOC in the soils dissolved, and the hydrophobic surface of the soils was digested, leading to reduced toluene adsorption (You et al., 1999). In contrast, low pH environments protonized the carboxyl group in TOC to form hydrophobic substances, which could adsorb toluene on hydrophobic surface groups (Adeyinka and Moodley, 2019). As such, the soils in the acid rain area exhibited a higher absorption capacity to toluene and HOPs (Adeyinka and Moodley, 2019).

Fig. 3b shows the relationship between the K_d of soils and their redox potentials. In the figure, soils A-F are natural soils, while soil A'-F' are their toluene adsorbed counterparts. A good linear correlation was found between redox potential and K_d in natural soils (r = 0.932, p = 2.05e-8 < 0.05). A slightly lower r (0.912) was found between K_d and redox potentials in adsorbed soils, and the p-value was 1.08e-9 < 0.05. Meanwhile, the lower redox potentials of adsorbed soils compared

to those of natural soils indicated that toluene adsorption reduced soil oxidation. Importantly, these results showed that soils with a strong adsorption capacity led to a significant potential difference before and after the toluene adsorption equilibrium, and this potential difference gradually decreased with the decline of K_d. These results were consistent with the observations in Fig. 3a, as the redox potentials in soils were also negatively related to soil pH.

Redox potential reflected the macroscopic redox property of soils, which was also critical in the formation and transformation of humus in the soil. The redox-active groups (quinone groups) of soil HA participate in the redox reaction via electron transfer (Scott et al., 1998; Struyk and Sposito, 2001). It is known that soil hydrophobicity increases with the number of quinone groups (González Pérez et al., 2004; Milori et al., 2002). For the soils with a high redox potential, the number of quinone groups in the soils was higher, resulting in stronger hydrophobic adsorption capacity, as indicated by Fig. 3b. Conversely, the decreased redox potential observed in soils that had toluene adsorption equilibrium was due to the decrease in the oxidability of quinone groups owing to the bonding between them and toluene. Therefore, the differences between the fitting curves before and after adsorption in Fig. 3b also reflect the amount of toluene adsorbed by quinone groups. That is, the greater the amount of toluene absorbed by quinone groups, the greater the decrease in redox potential; intuitively, the shaded portion representing the difference was distributed in a wedge (González Pérez et al., 2004).

Fig. 3c and Fig. 3d show correlations between K_d and zeta potential. In Fig. 3c, the K_d of soils exhibited linear increment (r=0.914, p=7.94e-4<0.05), when zeta potentials approached to neutral. It was consistent with K_d's correlation to pH shown in Fig. 3a, as zeta potential (negative) decreased with an increase in alkalinity. In Fig. 3d, the x-axis represents the differences of the zeta

potentials of soils before and after their toluene adsorption equilibrium (with coordinate points are expressed as △Soil A-F). A relatively good linear fit was also found (r = 0.888), indicating that the larger the toluene adsorption, the greater the zeta potential difference.

The zeta potential could reflect changes in soils' electrochemical characteristics when its electrical double layer (EDL) is influenced (Kaya and Yukselen, 2005). Zeta potential gradually approached neutral, as shown in Fig. 3c; this indicated the increase of surface hydrophobicity and instability of the soil colloid. Previous studies on phenanthrene adsorptions have indicated that unstable soil colloids exhibited higher adsorption capacities (Luo et al., 2008; Zhang et al., 2011). The difference in the zeta potentials before and after adsorption indicated that adsorption increased the thickness of the EDL and decreased the dielectric constant of the pore fluid (Goodarzi et al., 2016). This has also been observed in the adsorption of other HOPs, such as benzene and polycyclic aromatic hydrocarbons (PAHs) (Hunter, 1981; Lambert, 2018; Plaza et al., 2015).

4 Discussion

4.1 Mechanisms

The thermodynamic data (enthalpy) of toluene adsorption on various natural soils is provided in the Appendix (Table D.1). As the enthalpy values were all negative, the adsorption process was exothermic. The absolute values of enthalpy were all between 4.5-6.5 KJ/mol; this was close to the energy of hydrophobic interaction, hydrogen bonding and Van der Waals force shown in Table D.2 (Ngueleu et al., 2018; von Oepen et al., 1991). Therefore, the adsorption mechanisms may be these three forces. As described in Section 3.3.1, the effect of SSA on toluene adsorption was weak, indicating that the adsorption sites for toluene were not uniformly distributed. Therefore, specific adsorption sites and mechanisms needed to be clarified.

Based on adsorption thermodynamics and combined with all physicochemical properties, two main mechanisms that may be responsible for the adsorption behaviors of toluene on natural soils could be proposed: hydrophobic interaction and hydrogen-pi bonding (Lambert, 2018; Tolls, 2001).

First, hydrophobic surfaces such as siloxane surfaces, especially in clayey minerals, contribute to toluene adsorption via hydrophobic interactions (adsorption enthalpy, ~5 KJ/mol). The XRD results indicated that soils with a greater proportion of clayey minerals (or other minerals with intense activity) had better adsorption capacity, as there was a larger number of hydrophobic surfaces. Toluene being hydrophobic, its adsorption at hydrophobic sites was facilitated. Furthermore, in the FTIR results, the lower wavenumber of siloxane groups after adsorption also reflected the hydrophobic adsorption of toluene on soils. With the understanding of pH and redox potentials, these results demonstrated the presence of the hydrophobic interaction. This mechanism shows in Fig. 4a, toluene molecules adsorb on some surfaces due to the soil hydrophobicity caused by siloxane surfaces and other environmental variables. Particularly, the adsorption enthalpy was relatively low in the energy range of van der Waals force (4-10 KJ/mol), illustrating that the dispersion force, which may exist between nonpolar molecules, contributed substantially to toluene adsorption on hydrophobic sites (Jabraoui et al., 2019a; Jabraoui et al., 2019b). However, it should be noted that soils showed fewer adsorption capacities to toluene when the cations presented on the siloxane surface (Hunt et al., 1988; Lambert, 2018).

Second, the other mechanism was the weak hydrogen bonding determined by enthalpy. The adsorption enthalpy of each soil was small compared with the range for hydrogen bonding (2-40 KJ/mol), showing that the hydrogen bonding may be weak. And interestingly, based on the FTIR

results, although the lower wavenumber of the silanol and aluminol reflected toluene adsorption on these groups, these groups were polar and were not hydrophobic. Therefore, there must be a special mechanism, not only hydrophobic interaction. As shown in Fig. 4b, for toluene, a pi bond exists outside the benzene ring, which may provide electron donors (Keiluweit and Kleber, 2009; Parida et al., 2006). Meanwhile, the hydroxyl of polar groups (i.e., silanol and aluminol) can accept the electron donor (Jabraoui et al., 2019b). Therefore, the pi bond of toluene could combine with the silanol and aluminol groups to form hydrogen-pi bonding (O-H…pi) (Jabraoui et al., 2019b), causing toluene adsorbed on the soil surfaces. These bonding processes are well reflected in Fig. 4b. And the acid and alkali conditions could influence the weak hydrogen bond to change adsorption capacity, also reflecting the presence of this mechanism (Ertli et al., 2004).

Importantly, due to the hydrophilic nature of clayey minerals, the co-adsorption behavior of toluene and water must be considered. Whilst water molecules are preferentially adsorbed on the hydrophilic minerals (Yang et al., 2018), for some of the less polar surfaces and hydrophobic surfaces, partial toluene adsorption could still occur. More concretely, the co-adsorption of toluene and water molecules is shown in Fig. 4c. First, toluene molecules may be inserted into the water molecules layer (hydration layer), and even further adsorbed to soil surfaces due to hydrophobic/hydrogen bonding, which was the reason for the adsorption on the soil surfaces (inner layer) in Fig. 4c. Second, toluene molecules may co-occupy the diffusion layer with hydrated ions/water molecules (Lambert, 2018), showing the co-adsorption on the outer layer of Fig. 4c. Through these influences, co-adsorption would thicken the EDL. That was why toluene adsorption did not introduce new charges, but it influenced the zeta potential. The stronger the toluene adsorption, the higher the zeta potential. Therefore, the zeta potential difference showed a

good correlation with adsorption.

4.2 Weight analysis and modeling

Fig. H.1 in the Appendix presents the linear fitting only using the soil TOC (mg/g) as the *x*-axis and K_d (L/kg) as the *y*-axis. Fig. H.1 shows that there was a poor linear correlation (r=0.689) between the K_d and TOC. Some studies have also reported that the relationship was poor when the TOC content was close (Joo et al., 2011; Martz et al., 2019). In these cases, predicting the adsorption capacity of K_d using the TOC of soils may lead to a great deviation. Therefore, it was necessary to build a new model based on the impact of soil physicochemical properties on toluene adsorption and its mechanisms.

The results herein and the previously reported literature indicated that the adsorption of toluene on soils was dependent on TOC and other soil properties such as mineral composition, functional groups, pH, and zeta and redox potentials. Therefore, the importance of TOC and soil properties should be fully considered in the establishment of an adsorption capacity model to accurately describe adsorption behavior. However, it was impractical to adopt all these parameters in a complex model to correct the prediction deviation. Consequently, we proposed a model with deviation correction using two commonly used soil parameters: soil organic matter (SOM) and plastic limit (PL).

The PL is the limit moisture content when soils change from the plastic state to the semi-solid state, equivalent to the maximum bound water content of the soil, which reflects its capacity to combine with water (Wei et al., 2015). It is a crucial soil physical parameter that is used to describe and classify cohesive soils (Mitchell and Soga, 2005). The PL could quantitatively reflect the influence of many soil properties, such as mineral composition, pH, and potentials. For

example, the more clay in the mineral composition, the larger the PL; further, particle size and type of clayey minerals could also influence the PL (Andrade et al., 2011). The larger the zeta potentials, the thicker the EDL and the higher the PL (Liu et al., 2018). All these relationships would increase the adsorption capacity of toluene. Therefore, PL can roughly reflect the influence of various soil physicochemical properties, and it is reasonable to infer that a larger PL would provide more favorable conditions for toluene adsorption.

Meanwhile, previous studies have indicated a relationship between SOM and TOC, suggesting that the SOM contains TOC (Horwath, 2007; You et al., 1999). We used the SOM rather than TOC was because the SOM content in soils was easier to test rapidly and was more suitable for engineering applications (ASTM, 2014).

Table 4 shows the dimensionless soil parameters of PL, SOM, and determination factor (*DF*) that were used in the proposed model. As indicated in Table 4, PL and SOM were calculated by dividing the testing values of the six soils by the largest values. On the other hand, *DF* was a combination factor, including both PL and SOM, that determined using the entropy-weight method (Delgado and Romero, 2016; Fagbote et al., 2014; Ji et al., 2015). Its calculation is described in Formulas (I.1)-(I.4) of the Appendix.

Inputting the dimensionless data of SOM and PL into the formulas produced the weight of SOM (W_1=0.472), and the weight of the PL (W_2=0.528), respectively. According to dimensionless data and the calculated weight, the *DF* could be defined as per formula (1), used to easy and rapid determination of the adsorption behavior in engineering:

$$DF=\frac{\ln(\mathrm{SOM}\times W_1+\mathrm{PL}\times W_2)}{\mathrm{SOM}\times W_1+\mathrm{PL}\times W_2} \quad (1)$$

Previous studies have suggested that using logarithmic relationships resulted in better

correlations between K_d and the TOC of soils (Hur and Schlautman, 2004; Karickhoff et al., 1979; Payá-Pérez et al., 1992), as shown in Fig. J.1 and formula (J.1) of the Appendix for details. Therefore, *DF* was defined as the natural logarithm in formula (1) and as an independent variable in the new model. The dependent variable remained K_d; this was more conducive to comparing these models.

According to Fig. 5, a good linear correlation was observed in the relationship between K_d and *DF* (r=0.933, p=5.46e-10<0.05). The model is shown in formula (2). Compared to the linear correlation between K_d and TOC (Appendix, Fig. H.1), the r of this new model increased from 0.689 to 0.933, even when the TOC content range for the soils was close. Through obtaining the *DF*, this new model was able to provide good predictions on soil adsorption behaviors.

$$K_d=4.80+3.53DF \quad (2)$$

5 Conclusions

This study investigates toluene adsorption on natural soils with various physicochemical properties, analyzes the adsorption mechanisms, and establishes a model based on soil properties to precisely predict adsorption capacity. For low concentrations of toluene, the linear isothermal model provides a perfect fitting (R^2 = 0.958-0.994), where its coefficient, K_d, represents the adsorption capacity. First, soil properties, including mineral composition, functional groups, pH (r = 0.806), zeta potential (r = 0.914), and redox potential (r = 0.932), perfectly reflect toluene adsorption behaviors, while the SSA does not show the same (r = 0.0433). Second, adsorption mechanisms, such as hydrophobic interaction and hydrogen-pi bonding, are identified based on adsorption thermodynamics and the influences of soil properties. Meanwhile, co-adsorption is also observed between the toluene and water molecules. Finally, *DF* is derived considering all

properties, and a new model is established ($K_d = 4.80+3.53DF$). The new model is able to correct the deviation of TOC content as an independent variable and provide a more accurate prediction of K_d. The correlation of the model increases from $r = 0.689$ to $r = 0.933$. These results and analyses will provide new insights into toluene adsorption on natural soils.

Acknowledgments

This work was supported by the National Science Found for Distinguished Young Scholars (grant number 51625903); National Key Research and Development Project (grant number 2019YFC1804002); National Natural Science Foundation of China (grant number 51827814, 41702349, 41772342, 41977254); Youth Innovation Promotion Association CAS (grant number 2017376); Foundation for Innovative Research Groups of Hubei Province (grant number 2019CFA012); Wuhan science and technology conversion special project (grant number 2018060403011348); and Natural Science Foundation of Hubei Province (grant number 2017CFB203).

Special thanks to my best friends, Wei Zijun, Zhou Xinhui, Xu Zihao, Nie Pengbo. With their help, I have acquired many experimental soils that can reflect regional differences in China. Thanks for the experimental support provided by the Jiangsu Institute of Zoneco Co. Ltd.

References

Adeyinka, G.C., Moodley, B., 2019. Kinetic and thermodynamic studies on partitioning of polychlorinated biphenyls (PCBs) between aqueous solution and modeled individual soil particle grain sizes. J. Environ. Sci-China. 76, 100-110.

Agarwal, A., Liu, Y., 2015. Remediation technologies for oil-contaminated sediments. Mar. Pollut. Bull. 101, 483-490.

Andrade, F.A., Al-Qureshi, H.A., Hotza, D., 2011. Measuring the plasticity of clays: A review. Appl. Clay. Sci. 51, 1-7.

ASTM, 2014. Standard Test Methods for Moisture, Ash, and Organic Matter of Peat and Other Organic Soils, D2974-14. ASTM International, West Conshohocken.

Awad, A.M., Shaikh, S.M.R., Jalab, R., Gulied, M.H., Nasser, M.S., Benamor, A., Adham, S., 2019. Adsorption of organic pollutants by natural and modified clays: A comprehensive review. Sep. Purif. Technol. 228, 115719.

Balseiro-Romero, M., Monterroso, C., Casares, J.J., 2018. Environmental Fate of Petroleum Hydrocarbons in Soil: Review of Multiphase Transport, Mass Transfer, and Natural Attenuation Processes. Pedosphere 28, 833-847.

Bernier, M.-H., Levy, G.J., Fine, P., Borisover, M., 2013. Organic matter composition in soils irrigated with treated wastewater: FT-IR spectroscopic analysis of bulk soil samples. Geoderma 209-210, 233-240.

Carmo, A.M., Hundal, L.S., Thompson, M.L., 2000. Sorption of Hydrophobic Organic Compounds by Soil Materials: Application of Unit Equivalent Freundlich Coefficients. Environ. Sci. Technol. 34, 4363-4369.

Chen, D., Xing, B., Xie, W., 2007. Sorption of phenanthrene, naphthalene and o-xylene by soil organic matter fractions. Geoderma 139, 329-335.

Cheng, H., Song, Y., Bian, Y., Ji, R., Wang, F., Gu, C., Yang, X., Ye, M., Ouyang, G., Jiang, X., 2019. Meso-/microporous carbon as an adsorbent for enhanced performance in solid-phase microextraction of

chlorobenzenes. Sci. Total. Environ. 681, 392-399.

Chiou, C.T., Kile, D.E., Rutherford, D.W., Sheng, G., Boyd, S.A., 2000. Sorption of Selected Organic Compounds from Water to a Peat Soil and Its Humic-Acid and Humin Fractions: Potential Sources of the Sorption Nonlinearity. Environ. Sci. Technol. 34, 1254-1258.

Delgado, A., Romero, I., 2016. Environmental conflict analysis using an integrated grey clustering and entropy-weight method: A case study of a mining project in Peru. Environ. Modell. Softw. 77, 108-121.

Deng, L., Yuan, P., Liu, D., Annabi-Bergaya, F., Zhou, J., Chen, F., Liu, Z., 2017. Effects of microstructure of clay minerals, montmorillonite, kaolinite and halloysite, on their benzene adsorption behaviors. Appl. Clay. Sci. 143, 184-191.

Du, H., Miller, J.D., 2007. A molecular dynamics simulation study of water structure and adsorption states at talc surfaces. Int. J. Miner. Process. 84, 172-184.

Durand, C., Rosenberg, E., 1998. Fluid distribution in kaolinite- or illite-bearing cores: Cryo-SEM observations versus bulk measurements. J. Petrol. Sci. Eng. 19, 65-72.

Ertli, T., Marton, A., Foldenyi, R., 2004. Effect of pH and the role of organic matter in the adsorption of isoproturon on soils. Chemosphere 57, 771-779.

Essaid, H.I., Bekins, B.A., Cozzarelli, I.M., 2015. Organic contaminant transport and fate in the subsurface: Evolution of knowledge and understanding. Water. Resour. Res. 51, 4861-4902.

Fagbote, E.O., Olanipekun, E.O., Uyi, H.S., 2014. Water quality index of the ground water of bitumen deposit impacted farm settlements using entropy weighted method. Int. J. Environ. Sci. Te. 11, 127-138.

Flores, C., Morgante, V., Gonzalez, M., Navia, R., Seeger, M., 2009. Adsorption studies of the herbicide simazine in agricultural soils of the Aconcagua valley, central Chile. Chemosphere 74, 1544-1549.

Garoma, T., Skidmore, L., 2011. Modeling the influence of ethanol on the adsorption and desorption of selected

BTEX compounds on bentonite and kaolin. J. Environ. Sci-China. 23, 1865-1872.

Gholami, F., Mosmeri, H., Shavandi, M., Dastgheib, S.M.M., Amoozegar, M.A., 2019. Application of encapsulated magnesium peroxide (MgO2) nanoparticles in permeable reactive barrier (PRB) for naphthalene and toluene bioremediation from groundwater. Sci. Total. Environ. 655, 633-640.

Gondar, D., Lopez, R., Antelo, J., Fiol, S., Arce, F., 2013. Effect of organic matter and pH on the adsorption of metalaxyl and penconazole by soils. J. Hazard. Mater. 260, 627-633.

González Pérez, M., Martin-Neto, L., Saab, S.C., Novotny, E.H., Milori, D.M.B.P., Bagnato, V.S., Colnago, L.A., Melo, W.J., Knicker, H., 2004. Characterization of humic acids from a Brazilian Oxisol under different tillage systems by EPR, 13C NMR, FTIR and fluorescence spectroscopy. Geoderma 118, 181-190.

Goodarzi, A.R., Najafi Fateh, S., Shekary, H., 2016. Impact of organic pollutants on the macro and microstructure responses of Na-bentonite. Appl. Clay. Sci. 121-122, 17-28.

Horwath, W., 2007. 12 - Carbon cycling and formation of soil organic matter, in: Paul, E.A. (Eds.), Soil Microbiology, Ecology and Biochemistry (Third Edition). Academic Press, San Diego, pp. 303-339.

Hu, S., Zhang, Y., Shen, G., Zhang, H., Yuan, Z., Zhang, W., 2019. Adsorption/desorption behavior and mechanisms of sulfadiazine and sulfamethoxazole in agricultural soil systems. Soil. Till. Res. 186, 233-241.

Hunt, J.R., Sitar, N., Udell, K.S., 1988. Nonaqueous Phase Liquid Transport and Cleanup: 1. Analysis of Mechanisms. Water. Resour. Res. 24, 1247-1258.

Hunt, L.J., Duca, D., Dan, T., Knopper, L.D., 2019. Petroleum hydrocarbon (PHC) uptake in plants: A literature review. Environ. Pollut. 245, 472-484.

Hunter, R.J., 1981. 8 - Influence of More Complex Adsorbates on Zeta Potential, in: Hunter, R.J. (Eds.), Zeta Potential in Colloid Science. Academic Press, pp. 305-344.

Hur, J., Schlautman, M.A., 2004. Influence of Humic Substance Adsorptive Fractionation on Pyrene Partitioning to

Dissolved and Mineral-Associated Humic Substances. Environ. Sci. Technol. 38, 5871-5877.

Jabraoui, H., Hessou, E.P., Chibani, S., Cantrel, L., Lebegue, S., Badawi, M., 2019a. Adsorption of volatile organic and iodine compounds over silver-exchanged mordenites: A comparative periodic DFT study for several silver loadings. Appl. Surf. Sci. 485, 56-63.

Jabraoui, H., Khalil, I., Lebegue, S., Badawi, M., 2019b. Ab initio screening of cation-exchanged zeolites for biofuel purification. Mol. Syst. Des. Eng. 4, 882-892.

Ji, Y., Huang, G.H., Sun, W., 2015. Risk assessment of hydropower stations through an integrated fuzzy entropy-weight multiple criteria decision making method: A case study of the Xiangxi River. Expert. Syst. Appl. 42, 5380-5389.

Joo, J.C., Kim, J.Y., Nam, K., 2011. Sorption of nonpolar neutral organic compounds to model aquifer sands: Implications on blocking effect. J. Environ. Sci. Heal. A. 46, 1008-1019.

Karickhoff, S.W., Brown, D.S., Scott, T.A., 1979. Sorption of hydrophobic pollutants on natural sediments. Water. Res. 13, 241-248.

Kaya, A., Yukselen, Y., 2005. Zeta potential of soils with surfactants and its relevance to electrokinetic remediation. J. Hazard. Mater. 120, 119-126.

Keiluweit, M., Kleber, M., 2009. Molecular-Level Interactions in Soils and Sediments: The Role of Aromatic pi-Systems. Environ. Sci. Technol. 43, 3421-3429.

Lambert, J.-F., 2018. 7 - Organic pollutant adsorption on clay minerals, in: Schoonheydt, R., Johnston,C.T., Bergaya, F. (Eds.), Developments in Clay Science. Elsevier, Amsterdam, pp. 195–253.

Li, F., Fang, X., Zhou, Z., Liao, X., Zou, J., Yuan, B., Sun, W., 2019. Adsorption of perfluorinated acids onto soils: Kinetics, isotherms, and influences of soil properties. Sci. Total. Environ. 649, 504-514.

Li, Y., Gupta, G., 1994. Adsorption/desorption of hydrocarbons on clay minerals. Chemosphere 28, 627-638.

Liang, Z., Chen, S., Yang, Y., Zhou, Y., Shi, Z., 2019. High-resolution three-dimensional mapping of soil organic carbon in China: Effects of SoilGrids products on national modeling. Sci. Total. Environ. 685, 480-489.

Lim, M.W., Lau, E.V., Poh, P.E., 2016. A comprehensive guide of remediation technologies for oil contaminated soil - Present works and future directions. Mar. Pollut. Bull. 109, 14-45.

Liu, P., Wang, S., Ge, L., Thewes, M., Yang, J., Xia, Y., 2018. Changes of Atterberg limits and electrochemical behaviors of clays with dispersants as conditioning agents for EPB shield tunnelling. Tunn. Undergr. Sp. Tech. 73, 244-251.

Long, A., Zhang, H., Lei, Y., 2013. Surfactant flushing remediation of toluene contaminated soil: Optimization with response surface methodology and surfactant recovery by selective oxidation with sulfate radicals. Sep. Purif. Technol. 118, 612-619.

Luo, L., Zhang, S., Ma, Y., Christie, P., Huang, H., 2008. Facilitating Effects of Metal Cations on Phenanthrene Sorption in Soils. Environ. Sci. Technol. 42, 2414-2419.

Martz, M., Heil, J., Marschner, B., Stumpe, B., 2019. Effects of soil organic carbon (SOC) content and accessibility in subsoils on the sorption processes of the model pollutants nonylphenol (4-n-NP) and perfluorooctanoic acid (PFOA). Sci. Total. Environ. 672, 162-173.

Milori, D., Neto, L., Bayer, C., Mielniczuk, J., Bagnato, V., 2002. Humification degree of soil humic acids determined by fluorescence spectroscopy. Soil. Sci. 167, 739-749.

Mitchell, J.K., Soga, K., 2005. Fundamentals of Soil Behavior, third ed. John Wiley & Sons, Inc., Hoboken.

MOHURD, 2019. Standard for geotechnical testing method, GB/T50123-2019. China Planning Press, Beijing.

Mora, V.C., Madueno, L., Peluffo, M., Rosso, J.A., Del Panno, M.T., Morelli, I.S., 2014. Remediation of phenanthrene-contaminated soil by simultaneous persulfate chemical oxidation and biodegradation processes. Environ. Sci. Pollut. Res. Int. 21, 7548-7556.

Moyo, F., Tandlich, R., Wilhelmi, B.S., Balaz, S., 2014. Sorption of hydrophobic organic compounds on natural sorbents and organoclays from aqueous and non-aqueous solutions: a mini-review. Int. J. Env. Res. Pub. He. 11, 5020-5048.

Nayak, P.S., Singh, B.K., 2007. Instrumental characterization of clay by XRF, XRD and FTIR. B. Mater. Sci. 30, 235-238.

Ngueleu, S.K., Rezanezhad, F., Al-Raoush, R.I., Van Cappellen, P., 2018. Sorption of benzene and naphthalene on (semi)-arid coastal soil as a function of salinity and temperature. J. Contam. Hydrol. 219, 61-71.

Nguyen, T., Janik, L., Raupach, M., 1991. Diffuse reflectance infrared fourier transform (DRIFT) spectroscopy in soil studies. Soil Res. 29, 49-67.

Parida, S.K., Dash, S., Patel, S., Mishra, B.K., 2006. Adsorption of organic molecules on silica surface. Adv. Colloid. Interface. 121, 77-110.

Payá-Pérez, A.B., Cortés, A., Sala, M.N., Larsen, B., 1992. Organic matter fractions controlling the sorption of atrazine in sandy soils. Chemosphere 25, 887-898.

Pino-Herrera, D.O., Pechaud, Y., Huguenot, D., Esposito, G., van Hullebusch, E.D., Oturan, M.A., 2017. Removal mechanisms in aerobic slurry bioreactors for remediation of soils and sediments polluted with hydrophobic organic compounds: An overview. J. Hazard. Mater. 339, 427-449.

Plaza, I., Ontiveros-Ortega, A., Calero, J., Aranda, V., 2015. Implication of zeta potential and surface free energy in the description of agricultural soil quality: Effect of different cations and humic acids on degraded soils. Soil. Till. Res. 146, 148-158.

SAC, 2008. Chemicals—Adsorption-desorption using a batch equilibrium method, GBT21851-2008. China Planning Press, Beijing.

Scott, D.T., McKnight, D.M., Blunt-Harris, E.L., Kolesar, S.E., Lovley, D.R., 1998. Quinone Moieties Act as

Electron Acceptors in the Reduction of Humic Substances by Humics-Reducing Microorganisms. Environ. Sci. Technol. 32, 2984-2989.

Struyk, Z., Sposito, G., 2001. Redox properties of standard humic acids. Geoderma 102, 329-346.

Su, Y.H., Zhu, Y.G., Sheng, G., Chiou, C.T., 2006. Linear adsorption of nonionic organic compounds from water onto hydrophilic minerals: Silica and alumina. Environ. Sci. Technol. 40, 6949-6954.

Suanon, F., Tang, L., Sheng, H., Fu, Y., Xiang, L., Herzberger, A., Jiang, X., Mama, D., Wang, F., 2020. TW80 and GLDA-enhanced oxidation under electrokinetic remediation for aged contaminated-soil: Does it worth? Chem. Eng. J. 385, 123934.

Sun, J., Pan, L., Tsang, D.C.W., Zhan, Y., Zhu, L., Li, X., 2018. Organic contamination and remediation in the agricultural soils of China: A critical review. Sci. Total. Environ. 615, 724-740.

Sun, Y., Wang, J., Guo, G., Li, H., Jones, K., 2020. A comprehensive comparison and analysis of soil screening values derived and used in China and the UK. Environ. Pollut. 256, 113404.

Swartjes, F.A., Rutgers, M., Lijzen, J.P., Janssen, P.J., Otte, P.F., Wintersen, A., Brand, E., Posthuma, L., 2012. State of the art of contaminated site management in The Netherlands: policy framework and risk assessment tools. Sci. Total. Environ. 427-428, 1-10.

Tolls, J., 2001. Sorption of veterinary pharmaceuticals in soils: a review. Environ. Sci. Technol. 35, 3397-3406.

Vidonish, J.E., Zygourakis, K., Masiello, C.A., Sabadell, G., Alvarez, P.J.J., 2016. Thermal Treatment of Hydrocarbon-Impacted Soils: A Review of Technology Innovation for Sustainable Remediation. Engineering 2, 426-437.

von Oepen, B., Kördel, W., Klein, W., 1991. Sorption of nonpolar and polar compounds to soils: Processes, measurements and experience with the applicability of the modified OECD-Guideline 106. Chemosphere 22, 285-304.

Wei, M.L., Du, Y.J., Reddy, K.R., Wu, H.L., 2015. Effects of freeze-thaw on characteristics of new KMP binder stabilized Zn- and Pb-contaminated soils. Environ. Sci. Pollut. R. 22, 19473-19484.

Woolverton, P., Dragila, M.I., 2014. Characterization of hydrophobic soils: a novel approach using mid-infrared photoacoustic spectroscopy. Appl. Spectrosc. 68, 1407-1410.

Xing, B., 2001. Sorption of naphthalene and phenanthrene by soil humic acids. Environ. Pollut. 111, 303-309.

Xing, Z., Tian, K., Du, C., Li, C., Zhou, J., Chen, Z., 2019. Agricultural soil characterization by FTIR spectroscopy at micrometer scales: Depth profiling by photoacoustic spectroscopy. Geoderma 335, 94-103.

Xu, C., Lin, X., Yin, S., Liu, K., Liu, W., 2019. Spatio-vertical characterization of the BTEXS group of VOCs in Chinese agricultural soils. Sci. Total. Environ. 694, 133631.

Xu, L., Tian, J., Wu, H., Fang, S., Lu, Z., Ma, C., Sun, W., Hu, Y., 2018. Anisotropic surface chemistry properties and adsorption behavior of silicate mineral crystals. Adv. Colloid. Interface. 256, 340-351.

Yang, Y.L., Reddy, K.R., Du, Y.J., Fan, R.D., 2018. Sodium hexametaphosphate (SHMP)-amended calcium bentonite for slurry trench cutoff walls: workability and microstructure characteristics. Can. Geotech. J. 55, 528-537.

Ye, S., Zeng, G., Wu, H., Zhang, C., Liang, J., Dai, J., Liu, Z., Xiong, W., Wan, J., Xu, P., Cheng, M., 2017. Co-occurrence and interactions of pollutants, and their impacts on soil remediation—A review. Crit. Rev. Env. Sci. Tec. 47, 1528-1553.

Yin, X., Gupta, V., Du, H., Wang, X., Miller, J.D., 2012. Surface charge and wetting characteristics of layered silicate minerals. Adv. Colloid. Interface. 179-182, 43-50.

You, S.-J., Yin, Y., Allen, H.E., 1999. Partitioning of organic matter in soils: effects of pH and water/soil ratio. Sci. Total. Environ. 227, 155-160.

Zhang, L., Luo, L., Zhang, S., 2011. Adsorption of phenanthrene and 1,3-dinitrobenzene on cation-modified clay

minerals. Colloid. Surface. A. 377, 278-283.

Zytner, R.G., 1994. Sorption of benzene, toluene, ethylbenzene and xylenes to various media. J. Hazard. Mater. 38, 13-126.

Declaration of interests

☒ The authors declare that they have no known competing financial interests or personal relationships that could have appeared to influence the work reported in this paper.

☐The authors declare the following financial interests/personal relationships which may be considered as potential competing interests:

Yuan Li: Investigation, Data curation, Methodology, Writing - original draft. **Mingli Wei:** Conceptualization, Resources, Writing - review & editing. **Lei Liu:** Supervision, Writing - review & editing. **Qiang Xue:** Supervision, Resources Funding acquisition. **Bowei Yu:** Data Curation, Writing - review & editing.

Table 1. Basic physicochemical properties of six tested soils

Soil types	Physical properties							Chemical properties		Particle size distribution		
	Special gravity	TOC (mg/g)	Organic matter (%)	Plastic limit (%)	Plasticity index	SSA (m2/g)	Pore volume (cm^3/g)	pH	Zeta potential (mV)	Redox potential (mV)	Sand (>75 μm, %)	Silt (75-5 μm, %)	Clay (<5 μm, %)
A	2.23	12.3	5.09	20.4	16.6	20.2	0.03289	7.9	-12.9	199	70.8	22.7	6.5
B	2.75	14.1	5.88	25.7	19.7	14.1	0.05072	6.98	-1.72	260	74.9	16.5	8.6
C	2.69	14.6	5.92	24.9	15	13	0.05051	5.36	-1.24	283	89.6	7.5	2.9
D	2.78	9.36	4.73	22.3	25.7	27.6	0.053	7.06	-5.22	241	67.6	25.4	7
E	2.74	12.9	5.18	21.4	34.1	30.5	0.062	7.24	-12	231	81.2	15.2	3.6
F	2.68	8.43	4.73	19.8	12.5	15.9	0.02223	8.22	-16.9	190	64.4	27.3	8.3

Table 2. Fitting values of parameters in the adsorption isothermal model for each soil

Soil types	Freundlich isotherm					Linear isotherm		
	K_f		1/n		R^2	K_d		R^2
	Value	SD[a]	Value	SD[a]		Value	SD[a]	
A	4.70	0.0056	0.907	0.0413	0.901	3.92	0.0748	0.960
B	4.77	0.0632	0.990	0.0095	0.958	4.68	0.0773	0.982
C	7.07	0.0552	0.780	0.0163	0.921	4.67	0.0294	0.958
D	5.21	0.0259	0.920	0.0148	0.988	4.48	0.0356	0.994
E	4.90	0.0152	0.943	0.0160	0.983	4.40	0.0510	0.993
F	6.36	0.0738	0.717	0.0073	0.991	3.54	0.0962	0.986

NOTE: The expression and introduction of adsorption isotherm models are shown in the appendix (Table E.1)

[a] Standard deviation

Table 3. Quantitative analysis results of the main mineral composition of six soils (%)

Soil types	Clayey minerals			Non-clayey minerals				
	Kaolinite	Nacrite	Rectorite	Quartz	Microcline	Albite	Birnessite	Phosphide
A	/	/	/	81.2	/	18.8	/	/
B	69.4	/	/	/	30.6	/	/	/
C	/	79.3	/	20.7	/	/	/	/
D	/	/	24.8	72.7	/	/	2.5	/
E	/	/	/	68.4	/	29.2	/	2.4(Ti)
F	/	/	/	67.3	/	8.9	/	23.8(Ca)

NOTE: Combined with the spectra of Fig. 1, The processes of quantitative analysis are shown in the appendix (Fig. F.1-F.6). It is strictly a semi-quantitative analysis through PDF 2004 database

Table 4. Dimensionless parameters necessary for building the new model

Soil types	PL	SOM	*DF*
A	0.794	0.86	-0.206
B	1	0.993	-0.0049
C	0.969	1	-0.009
D	0.93	0.816	-0.194
E	0.852	0.875	-0.162
F	0.77	0.799	-0.297

NOTE: By calculating the weights of dimensionless numbers PL and SOM (Appendix, part I), DF is obtained based on the formula (1).

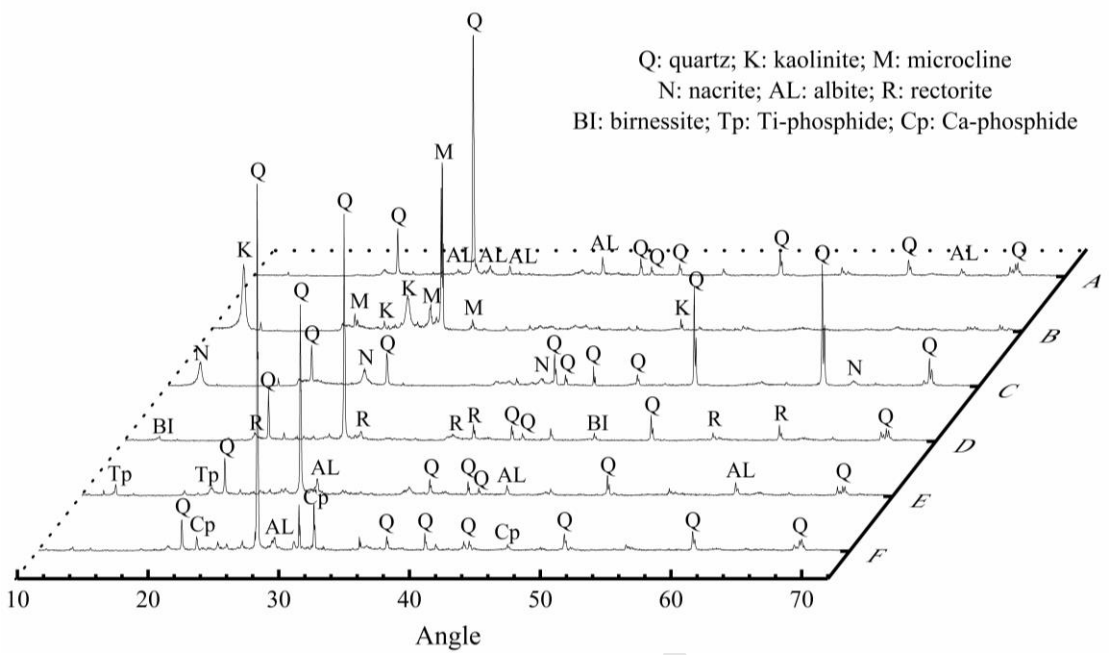

Figure 1. XRD spectra and main mineral composition of six soils (before adsorption)

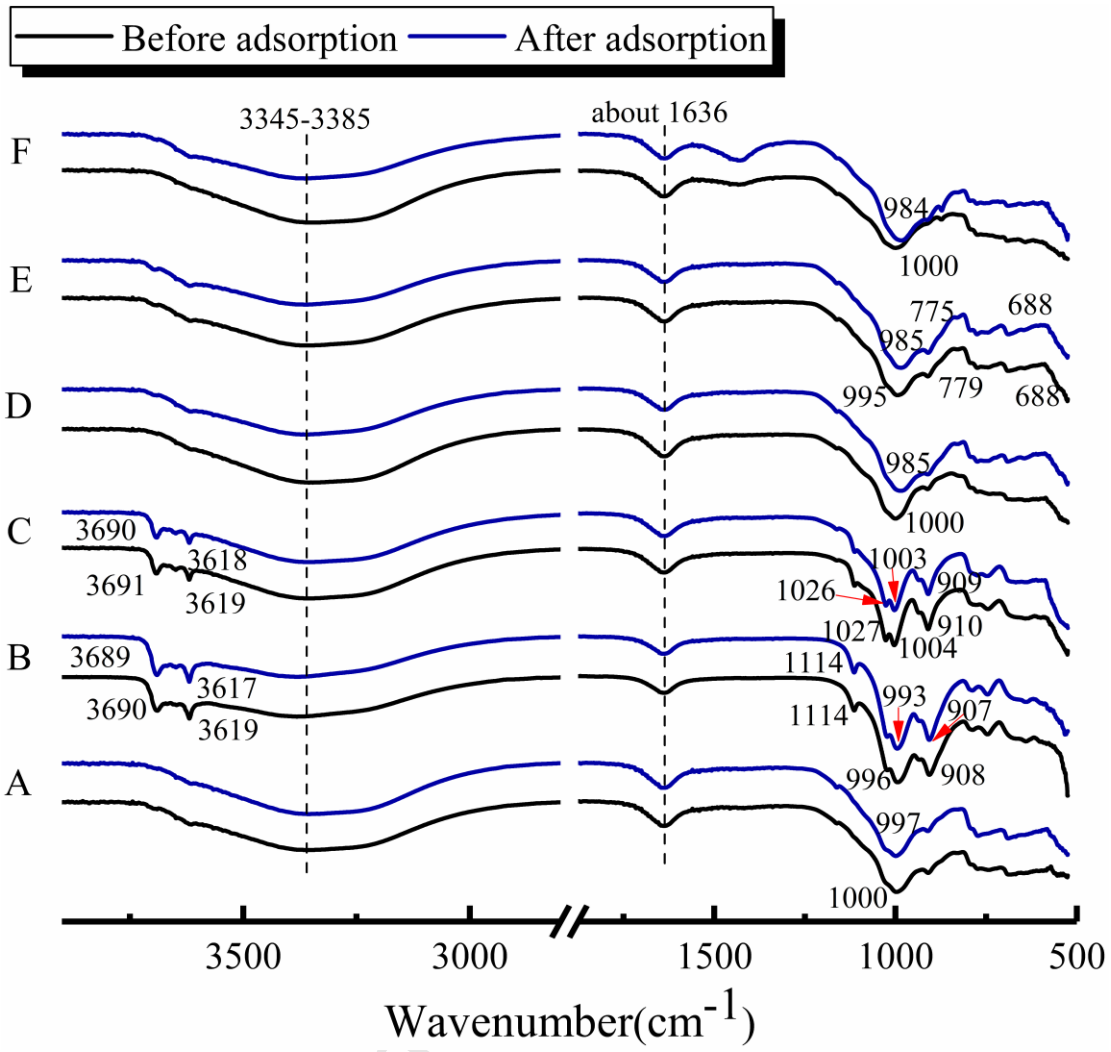

Figure 2. FTIR spectra of six soils before and after adsorption and their comparison

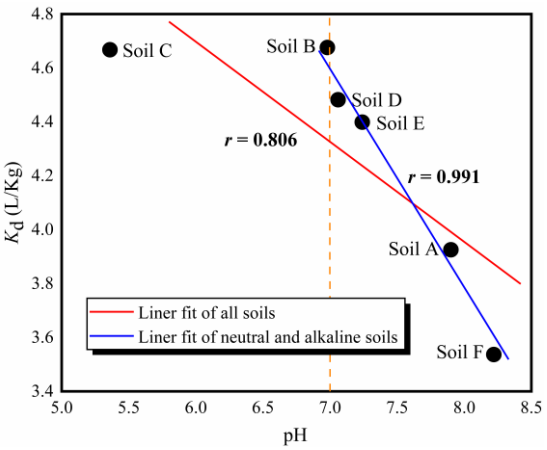

(a) pH of before adsorption

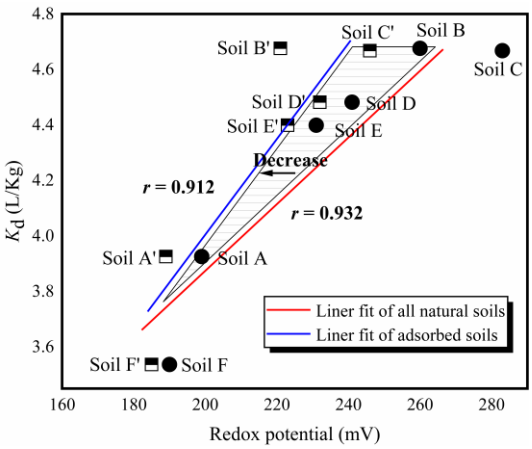

(b) Comparison of redox potential before and after adsorption

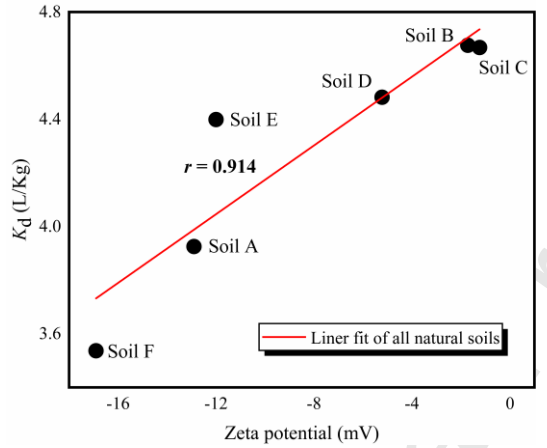

(c) Zeta potential of before adsorption

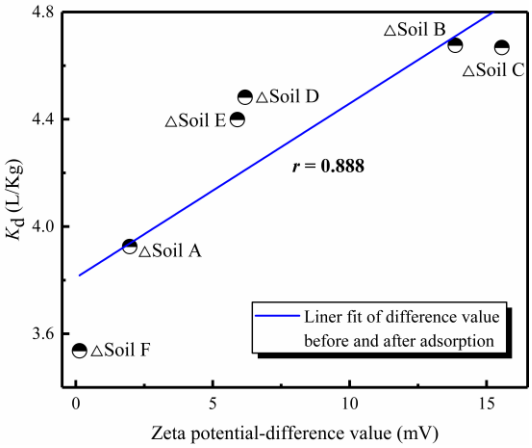

(d) Difference of zeta potential before and after adsorption

Figure 3. The relationship of soil's K_d and their chemical properties (pH, redox potential, zeta potential)

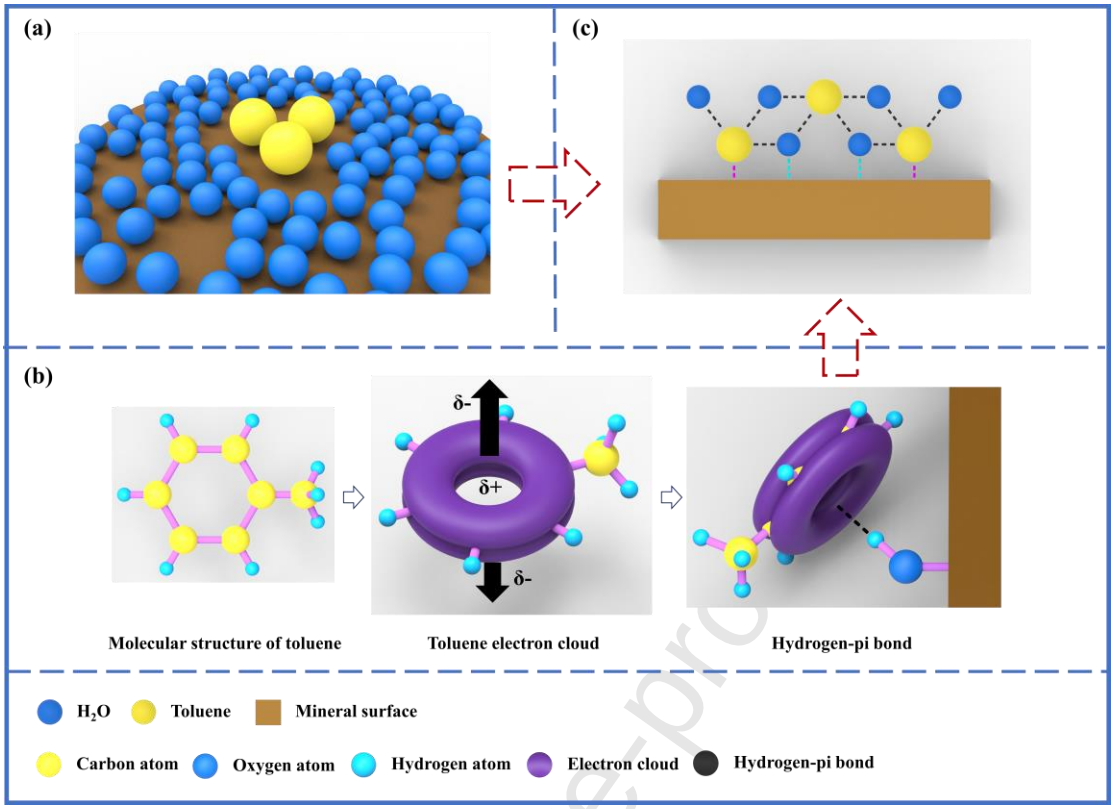

Figure 4. Adsorption mechanisms of toluene on the natural soil surface (a. hydrophobic interaction, b. hydrogen-pi bonding, c. co-adsorption)

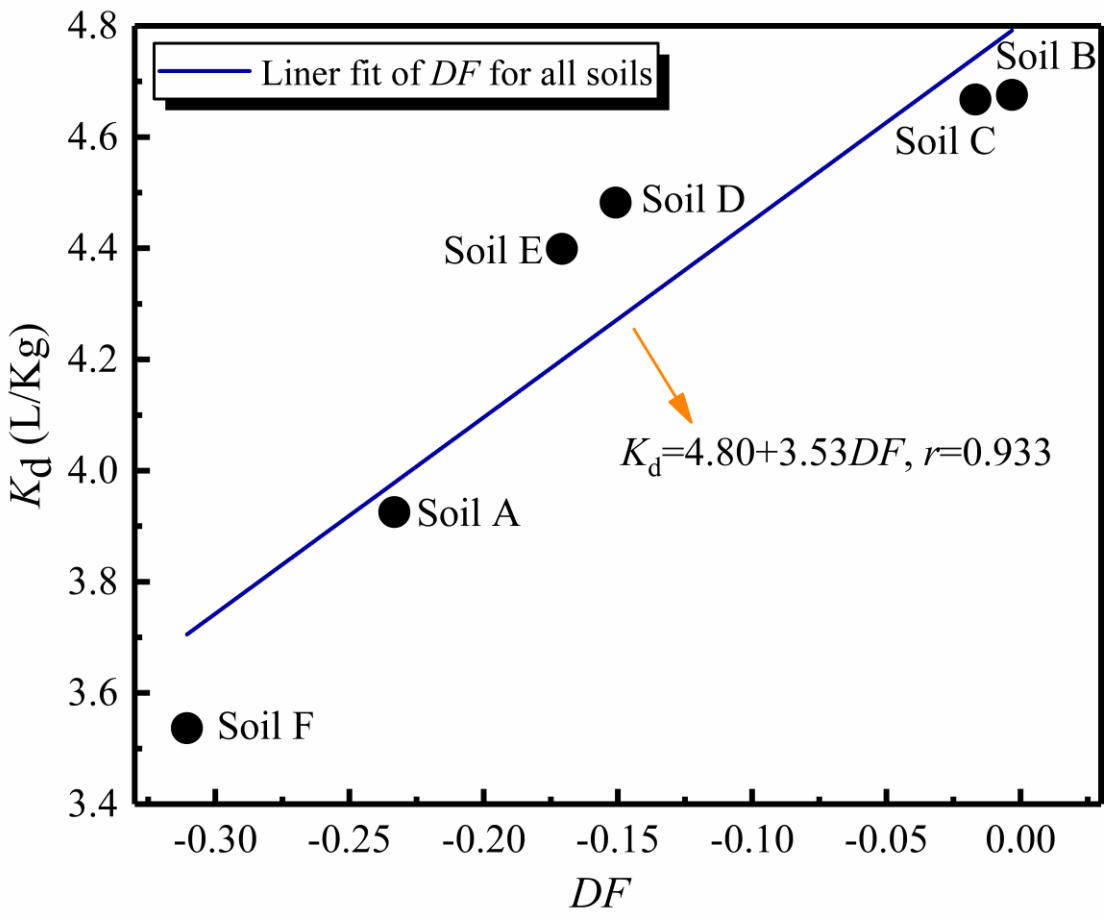

Figure 5. The new model of K_d-determination factor (*DF*)

Graphical abstract

Highlight：

- Soil properties are correlated to K_d of the linear isothermal model.
- Hydrogen-pi bonding is a unique adsorption mechanism than hydrophobic interaction.
- Toluene and water molecules co-adsorb on the hydration layer.
- Using PL & SOM to build *DF* which reflects the adsorption behavior of natural soils.
- Adsorption model based on *DF* can correct the deviation caused by TOC only.